Belantamab Mafodotin (GSK2857916) Drives Immunogenic Cell Death and Immune-mediated Antitumor Responses *In Vivo*

Rocio Montes de Oca[1], Alireza S. Alavi[2], Nick Vitali[2], Sabyasachi Bhattacharya[2], Christina Blackwell[2], Krupa Patel[2], Laura Seestaller-Wehr[2], Heather Kaczynski[2], Hong Shi[2], Eric Dobrzynski[3], Leslie Obert[4], Lyuben Tsvetkov[2], David C. Cooper[5], Heather Jackson[2], Paul Bojczuk[2], Sabrina Forveille[6,7], Oliver Kepp[6,7], Allan Sauvat[6,7], Guido Kroemer[6,7,8,9,10], Mark Creighton-Gutteridge[11], Jingsong Yang[2], Chris Hopson[2], Niranjan Yanamandra[2], Christopher Shelton[2], Patrick Mayes[2], Joanna Opalinska[12], Mary Barnette[2], Roopa Srinivasan[1], James Smothers[2], and Axel Hoos[12]

ABSTRACT

B-cell maturation antigen (BCMA) is an attractive therapeutic target highly expressed on differentiated plasma cells in multiple myeloma and other B-cell malignancies. GSK2857916 (belantamab mafodotin, BLENREP) is a BCMA-targeting antibody–drug conjugate approved for the treatment of relapsed/refractory multiple myeloma. We report that GSK2857916 induces immunogenic cell death in BCMA-expressing cancer cells and promotes dendritic cell activation *in vitro* and *in vivo*. GSK2857916 treatment enhances intratumor immune cell infiltration and activation, delays tumor growth, and promotes durable complete regressions in immune-competent mice bearing EL4 lymphoma tumors expressing human BCMA (EL4-hBCMA). Responding mice are immune to rechallenge with EL4 parental and EL4-hBCMA cells, suggesting engagement of an adaptive immune response, immunologic memory, and tumor antigen spreading, which are abrogated upon depletion of endogenous $CD8^+$ T cells. Combinations with OX40/OX86, an immune agonist antibody, significantly enhance antitumor activity and increase durable complete responses, providing a strong rationale for clinical evaluation of GSK2857916 combinations with immunotherapies targeting adaptive immune responses, including T-cell–directed checkpoint modulators.

Introduction

Although many neoplasms are eliminated by the immune system, some tumors can develop when malignant cells evade immune surveillance mechanisms. Tumor immune escape can be mediated by multiple factors including immunosuppressive factors within the tumor microenvironment and negative regulators that inhibit T-cell activity and promote tolerance (1). Modulation of such checkpoints by inhibitory mAbs against CTLA-4 and PD-1 has been associated with clinically significant responses in a variety of cancers (2). Moreover, agonism of costimulatory receptors such as OX40, upregulated on naïve and memory T cells following T-cell receptor ligation, significantly enhances T-cell proliferation and survival and differentiation to a memory phenotype, which may provide additional therapeutic benefit (3). Current efforts are focused on improving the clinical efficacy of immunotherapies through combinations with other checkpoint modulators, immunogenic chemotherapeutics, and radiotherapy (4–6).

A subset of chemotherapeutics has been shown to contribute to immune stimulation through antigen release secondary to cytotoxic cell death (7). Although normal apoptosis is nonimmunogenic, treatment with selected chemotherapeutics, such as anthracyclines and oxaliplatin, induces a unique form of cell death termed immunogenic cell death (ICD). ICD is characterized by the induction of the endoplasmic reticulum (ER) stress response and the exposure and/or release of danger-associated molecular patterns (DAMPs), many of which are Toll-like receptor ligands (8). After ICD induction, calreticulin, a DAMP molecule normally found in the ER lumen, is translocated to the surface of the dying cell, where it functions as an "eat me" signal for immature dendritic cells (DC; ref. 9). Other important DAMPs are HSPs, namely, HSP70 and HSP90, the secreted amphoterin high mobility group box 1 (HMGB1) protein, and extracellular adenosine triphosphate (ATP). ATP functions as a chemoattractant recruiting antigen-presenting cells (APCs) by interacting with purinergic receptors, whereas HMGB1 is considered a late apoptotic

[1]Experimental Medicine Unit, Oncology R&D, GlaxoSmithKline, Collegeville, Pennsylvania. [2]Immuno-Oncology and Combinations RU, Oncology R&D, GlaxoSmithKline, Collegeville, Pennsylvania. [3]Bioanalysis, Immunogenicity and Biomarkers, GlaxoSmithKline, Collegeville, Pennsylvania. [4]Translational Medicine and Comparative Pathobiology, GlaxoSmithKline, Collegeville, Pennsylvania. [5]Research Statistics, GlaxoSmithKline, Collegeville, Pennsylvania. [6]Equipe labellisée par la Ligue contre le cancer, Université de Paris, Sorbonne Université, INSERM U1138, Centre de Recherche des Cordeliers, Paris, France. [7]Metabolomics and Cell Biology Platforms, Gustave Roussy Cancer Center, Villejuif, France. [8]Pôle de Biologie, Hôpital Européen Georges Pompidou, AP-HP, Paris, France. [9]Suzhou Institute for Systems Medicine, Chinese Academy of Medical Sciences, Suzhou, P.R. China. [10]Karolinska Institute, Department of Women's and Children's Health, Karolinska University Hospital, Stockholm, Sweden. [11]Cell Therapy RU, Oncology R&D, GlaxoSmithKline, Hertfordshire, United Kingdom. [12]Oncology R&D, GlaxoSmithKline, Collegeville, Pennsylvania.

Note: Supplementary data for this article are available at Molecular Cancer Therapeutics Online (http://mct.aacrjournals.org/).

Corresponding Author: Rocio Montes de Oca, Experimental Medicine Unit, Oncology R&D, GlaxoSmithKline (United States), 1250 S. Collegeville Road, Collegeville, PA 19426. Phone: 610-917-5746; E-mail: maria-del-rocio.x.montes-de-oca-ruiz@gsk.com

Mol Cancer Ther 2021;20:1941–55

doi: 10.1158/1535-7163.MCT-21-0035

marker, and its release to the extracellular space seems to be required for the optimal release and presentation of tumor antigens to DCs, DC maturation, and synthesis of proinflammatory molecules including type I interferons (IFNs; refs. 10, 11). Furthermore, exposure of DCs to tumor cells undergoing ICD evokes an inflammatory phenotype (innate response), including an increase in costimulatory markers CD86 and MHC class II antigens and the activation of NFκB, a proinflammatory transcription factor complex (10). Mature DCs play a key role in priming robust immune responses in tumor-bearing hosts, and ICD can induce an effective antitumor immune response through DC activation and subsequent activation of tumor antigen-specific T-cell responses. Therapeutic approaches that activate DCs and promote tumor antigen-specific T-cell priming are needed to enhance the immunogenicity of tumors. In this regard, several chemotherapeutic agents and potent tubulin inhibitors, such as vinblastine and the auristatin analogs dolastatin 10 and monomethyl auristatin-E and -F (MMAE and MMAF, respectively), have been recently identified as potent activators of DC maturation and antigenic responses (12–14).

B-cell maturation antigen is a transmembrane receptor. Its normal function is to promote the survival of cells in the B-cell lineage, by transduction of signals from two known ligands from the tumor necrosis factor family: B-cell activating factor (BAFF/BLyS) and a proliferation-inducing ligand (APRIL). BCMA expression is restricted to B cells at later stages of differentiation, including germinal center B cells in tonsil, blood plasma blasts, and long-lived plasma cells (15). BCMA is also expressed in various B-cell malignancies including multiple myeloma, diffuse large B-cell lymphoma, large B-cell lymphoma, chronic lymphocytic leukemia, and Waldenström macroglobulinemia, at varying frequencies (16–19). BCMA's restricted normal tissue expression profile and upregulation and survival function in multiple myeloma and other B-cell malignancies, make it an attractive target for a therapeutic antibody with direct cell killing activity.

Belantamab mafodotin also known as GSK2857916 is a humanized, IgG1 antibody-drug conjugate (ADC) that binds specifically to BCMA (20). The parent anti-BCMA antibody (GSK2857914) is produced in an afucosylated form and is conjugated to the microtubule polymerization inhibitor MMAF, via a protease-resistant maleimidocaproyl (mc) linker, to produce the GSK2857916 ADC molecule. Upon binding to the cell surface, GSK2857916 is rapidly internalized and active cytotoxic drug (cys-mcMMAF) is released inside the cell causing cell-cycle arrest and apoptosis. Furthermore, the afucosylation of GSK2857916 leads to enhanced binding to FcγRIIIa receptors on the surface of immune effector cells, recruitment of immune cells, and antibody-dependent cellular cytotoxicity and phagocytosis (ADCC and ADCP, respectively). This dual mechanism of action enables improved efficacy by targeting both dividing (via ADC) and non-dividing (via ADCC/ADCP) tumor cells (21). Recently, belantamab mafodotin was approved under the name BLENREP in the United States and European Union for the treatment of patients with relapsed or refractory multiple myeloma.

Previous preclinical studies linked the direct cytotoxic activity of auristatin-class ADCs (e.g., dolastatins and brentuximab vedotin) to substantial therapeutic efficacy, by augmenting host immunity through direct effects on DC maturation and activation of antigen specific T cells, in addition to direct tumor cell killing (22, 23). In this study, we provide evidence that GSK2857916 potently induces prominent ICD markers and DC maturation and activation *in vitro*. In a syngeneic mouse model, GSK2857916 induced ICD, promoted intratumoral enrichment of tumor-infiltrating lymphocytes (TILs), and T-cell–dependent antitumor activity. Our data reveal a novel immune-mediated mechanism of action for GSK2857916, which is significantly enhanced in combination with an agonistic OX86 (mouse OX40) antibody, and provides rationale for the investigation and development of clinical combinations with GSK2857916 and immune checkpoint modulators.

Materials and Methods

Belantamab mafodotin or GSK2857916

GSK2857916 is a humanized, IgG1 mAb known as GSK2857914 (clone J6M0), which is derived from the murine mAb clone CA8, conjugated to MMAF. The CA8 murine heavy and light chain variable region amino acid sequences are provided as SEQ ID NO. 7 and SEQ ID NO. 9, respectively, in the published U.S. patent 9,273,141 B2. GSK2857916 is comprised of the CA8 humanized heavy (CA8 Humanized V_H J6) and light (CA8 Humanized V_L M0) chain variable region amino acid sequences provided as SEQ ID NO. 23 and SEQ ID NO. 31, respectively, of the same patent.

Cell lines

NCI-H929 cells were purchased and grown as per ATCC. The EL4-Luc-2-hBCMA cell line was generated by electroporating a plasmid encoding the human BCMA (hBCMA) receptor (residues 1–184) into the Bioware Ultra Cell Line EL4-luc2 [Caliper Life Sciences, Inc., catalog No. 124088, derived from (TIB-39)]. The EL4 parental (ATCC, catalog No. TIB-39) and EL4-hBCMA cells were grown in DMEM High Glucose (1×) + GlutaMAX (Gibco; catalog No. 10564-011 or 11965-092) with 10% FBS (Sigma-Aldrich; catalog No. 12176C) ± 200 μg/mL G418/Geneticin (Gibco; catalog No. 10131-027) at 37°C with 5% CO_2. Cells were used within <5 passages from day of thaw for experiments. Cells were authenticated by short tandem repeat profiling and were negative for *Mycoplasma*.

In vitro evaluation of cell viability, calreticulin exposure, and HMGB1 and ATP release in NCI-H929 multiple myeloma cells

NCI-H929 cells were left untreated or were exposed to GSK2857916 as indicated for 48 hours. Mitoxantrone (1 μmol/L; Sigma-Aldrich; catalog No. M6545), a known ICD inducer (9), was the positive control. Cell viability was assessed by automated flow cytometry. Cell surface calreticulin was analyzed in nonpermeabilized cells by flow cytometry (Abcam, catalog No. ab2907; diluted 1:100) with the fluorescence intensity of stained cells gated on propidium iodide (PI) negative cells. Extracellular HMGB1 concentrations were analyzed using an enzyme-linked immunosorbent assay (ELISA; Shino Test Corp ELISA kit II). Analysis of extracellular ATP content was by the ENLITEN ATP Assay system (Promega Corp, catalog No. FF2000). Secreted ATP was stabilized using an ectoATPase inhibitor (3 μmol/L ARL 67156 trisodium salt hydrate; Sigma-Aldrich, catalog No. A265). For all measurements, mean ± SD of triplicates from a representative experiment shown.

In vitro evaluation of additional hallmarks of ICD

Cells (5×10^5 cells/mL) were left untreated or exposed to the indicated treatments for the indicated time. Cells were counted on a Vi-Cell-XR Cell Viability Analyzer (Beckman Coulter).

For immunoblot analyses, cells were lysed using Cell Lysis Buffer (Cell Signaling Technology; catalog No. 9803) with a protease inhibitor cocktail (Roche; catalog No. 11873580001), and probed with the following antibodies: Phospho-PERK (Abcam; catalog No. ab192591; 1:1,000), PERK (R&D Systems; catalog No. AF3999; 1:200), phospho-

eIF2α (Cell Signaling Technology; catalog No. 3398S; 1:1,000), eIF2α (Cell Signaling Technology; catalog No. 2103S; 1:1,000), BAP31 (Cell Signaling Technology; catalog No. 4043S; 1:1,000), and GAPDH (Bethyl Laboratories; catalog No. A300-641A; 1:10,000).

ICD markers were quantified from cell supernatants by the following ELISAs: HSP70 (R&D Systems; catalog No. DYC1663-2; 1:2 sample dilution), HSP90α (Invitrogen; catalog No. BMS2090; 1:25 sample dilution), IL8 (R&D Systems; catalog No. D8000C; undiluted sample), mouse calreticulin (LifeSpan BioSciences; catalog No. LS-F6663; 1:10 or 1:15 sample dilution), HMGB1 (IBL International Corp; catalog No. ST51011; 1:4 sample dilution) and mouse HSPD1/HSP60 (LifeSpan Biosciences; catalog No. LS-F4239; undiluted sample).

Cell surface ICD markers were analyzed in nonpermeabilized cells by flow cytometry with the following antibodies or isotypes (at 0.7 mg/mL per reaction): anti-calreticulin mouse IgG2a (Novus; catalog No. NBP1-47518AF488), mouse IgG2a (R&D systems; catalog No. IC003G), anti-HSP90 mouse IgG1a (Novus; catalog No. NB100-1972AF488), mouse IgG1a (Novus; catalog No. DDXCM01A488), anti-HSP70/HSPA1A rabbit IgG (Novus; catalog No. NBP1-77455AF488), anti-HMGB1/HMG-1 rabbit IgG (Novus; catalog No. NB100-2322AF488) or rabbit IgG (Novus; catalog No. NBP2-24982), per manufacturer's instructions. Fluorescence intensity of stained cells was gated on live cells using Aqua Live Dead stain (Thermo Fisher Scientific; catalog No. L34957). Cells were acquired on a BD LSR Fortessa X-20 and analyzed by FlowJo software (v10.1r5; FlowJo, LLC).

In vitro activation of immature DCs by GSK2857916-treated NCI-H929 cells

Human blood was obtained from three healthy donors from the GlaxoSmithKline Blood Donation Unit using heparin-coated syringes. Monocytes were isolated from this blood using the RosetteSep Monocyte Enrichment kit (STEMCELL Technologies; catalog No. 15068) and were assessed for CD14 cell surface expression (BD Biosciences; catalog No. 562698) by flow cytometry. Isolated monocytes (1.5×10^6 cells/well) were cultured in 2 mL of X-Vivo-15 Media (Lonza; catalog No. BE02-054Q) supplemented with 1% autologous plasma, 250 ng/mL recombinant human GM-CSF (R&D Systems; catalog No. 215-GM-050) and 100 ng/mL recombinant human IL4 (R&D Systems; catalog No. 204-IL-050) for 7 days at 37°C and 5% CO_2. Cultures received a half media change on day 3 or 4 while maintaining stimulation factor concentrations. In parallel, NCI-H929 cells were plated at a density of 7.5×10^5 cells/mL in 2 mL, in 12-well plates, and were left untreated or were treated with GSK2857916 (0.1, 1, or 10 μg/mL) or hIgG1-MMAF (10 μg/mL) for 48 hours. On day 7, immature DCs derived from the monocytes were co-cultured with the treated NCI-H929 cells at a 1:1 ratio for 24 hours, in 96-well plates, 7.5×10^4 cells were seeded per well (100 μL). A flow cytometry panel consisting of CD1a (BD Biosciences; catalog No. 563938), CD11c (BD Biosciences; catalog No. 561355), CD40 (BD Biosciences; catalog No. 555751), CD80 (BD Biosciences; catalog No. 561135), CD83 (BD Biosciences; catalog No. 562630), CD86 (BD Biosciences; catalog No. 555657), HLA-DR (BD Biosciences; catalog No. 340591), and CD14 (BD Biosciences; catalog No. 562698) was used to assess DC differentiation and maturation on a BD FACS Canto II. These data were analyzed by FlowJo software (v7.6.5; FlowJo, LLC).

In vitro growth death assays

Cells were plated (1×10^4 cells/mL) in a 96-well format. On assay day 0, cells were treated in quadruplicate with a 12-point, three- or four-fold dilution series of GSK2857916, GSK2857914, MMAE (SAFC; catalog No. SGD-1010), vinorelbine (Sigma-Aldrich; catalog No. V2264) or colchicine (Sigma-Aldrich; catalog No. C9754), as indicated, for 3 days. Cell growth was evaluated on days 0 and 3 by CellTiter-Glo reagent (Promega; catalog No. G8462) and luminescence analysis. Dose–response curves, IC_{50} values and sensitivity between cell lines [% growth (mean ± S.D. of biological quadruplicates)] were calculated.

In vivo efficacy studies

Female C57/BL6 mice (8–10 weeks old from Charles River Laboratories) were injected subcutaneously in the right flank with EL4 parental or EL4-hBCMA cells harvested during exponential growth (1 or 3×10^5 cells in 0.1 mL). Tumor growth was monitored and tumor length (L) and width (W) were measured (in mm) to determine tumor volume ($L \times W^2/2$). Mice were randomized into groups and treatment began when average tumor volume was approximately 150–250 mm^3, or as indicated. Antibodies were administered by intraperitoneal injection twice weekly for 3 weeks for a total of six doses (or as indicated) and were well tolerated at all doses. Tumor volumes >2,000 mm^3 for an individual mouse resulted in euthanization.

Therapeutic efficacy was determined by calculating tumor burden for all mice over the course of the study by taking the area under the curve of tumor volume over time using the trapezoidal method. Adjusted area under the curve values for all mice in each group were analyzed by a nonparametric ANOVA (on the ranks). Furthermore, incidence, magnitude, and durability of regression responses were also evaluated. An animal with a complete regression response (CR = TV < 13.5 mm^3 for three consecutive measurements) at the termination of a study was classified as a tumor-free survivor. For rechallenge studies, tumor-free survivors were rechallenged on the flank opposite to the original implant side. Survival was analyzed by the Kaplan–Meier method.

Immunophenotyping by flow cytometric analysis

Isolated tumor cells were incubated with human or mouse FcR Blocking Reagent (Miltenyi Biotec; catalog No. 130-059-901 or 130-092-575, respectively) and Live/Dead stain (Thermo Fisher Scientific), then with antibodies directed against surface antigens for 30 minutes at 4°C as follows: anti-CD3 (145-2C11; catalog No. 553062), anti-CD4 (RM4-5; catalog No. 550954), anti-CD8 (53-6.7; catalog No. B560182), anti-CD25 (PC61; catalog No. 552880), anti-CD11c (HL3; catalog No. 560584), and anti-CD86 (GL1; catalog No. 553691), all from BD Biosciences. Anti-Granzyme B (GB11; catalog No. 12-8899-41) and anti-FoxP3 (FJK-16s; catalog No. 17-5773-82), from eBiosciences. Anti-human CD269 BCMA (19F2; catalog No. 357504), anti-Ki67 (16A8; catalog No. 652411), anti-PD-1 (RMP1-30; catalog No. 109110), anti-ICOS (C398.4A; catalog No. 313524), anti-CD69 (H1.2F3; catalog No. 104528), anti-CD49b (DX5; catalog No. 108908), anti-CD3 (17A2; catalog No. 100228), anti-CD4 (RM4-4; catalog No. 116004), anti-CD8 (53-5.8; catalog No. 140410), from BioLegend. Anti-OX40 (OX86; catalog No. FAB1256P) from R&D Systems. Anti-calreticulin (1G6A7; catalog No. NBP1-47518AF488) from Novus. Cell surface stains were followed by 2% paraformaldehyde for 20 minutes, washed and resuspended in Stain buffer (BD Pharmingen; catalog No. 554657). For intracellular staining, cells were incubated with fixation/permeabilization buffer (BD Biosciences; catalog No. 554714) for 30 minutes, followed by incubation with antibodies directed against intracellular antigens for an additional 30 minutes, washed and resuspended in stain buffer. Cells were acquired on a BD LSR Fortessa X-20 and data were analyzed by FlowJo software (v10.1r5; FlowJo, LLC).

NanoString analysis

NanoString analysis was performed on RNA (100 ng) extracted from dissociated tumor samples using the NanoString Mouse PanCancer Immune profiling panel (NanoString; catalog No. XT-CSO-MIP1-12). Data analysis was performed using nSolver 2.6 and the mouse PanCancer Immune advanced analysis software. The type I IFN-related signature was defined by the following genes: *Ccl2, Ccl3, Ccl4, Ccl7, Cd274, Cd69, Cxcl1, Cxcl10, Ifit2, Ifnb1, Il12a, Il12b, Irf3, Irf7, Mx1, Mx2, Oas2, Oasl1, Rsad2, Stat4*, and *Tnfrsf9* (modified from ref. 24).

IHC analysis

Mice were injected subcutaneously with EL4-hBCMA cells (1×10^6 cells in 0.1 mL). When tumors averaged a volume of approximately 800 mm^3, mice were randomized and dosed intraperitoneally with 15 mg/kg GSK2857916 or GSK2857914, as described. Tumors were

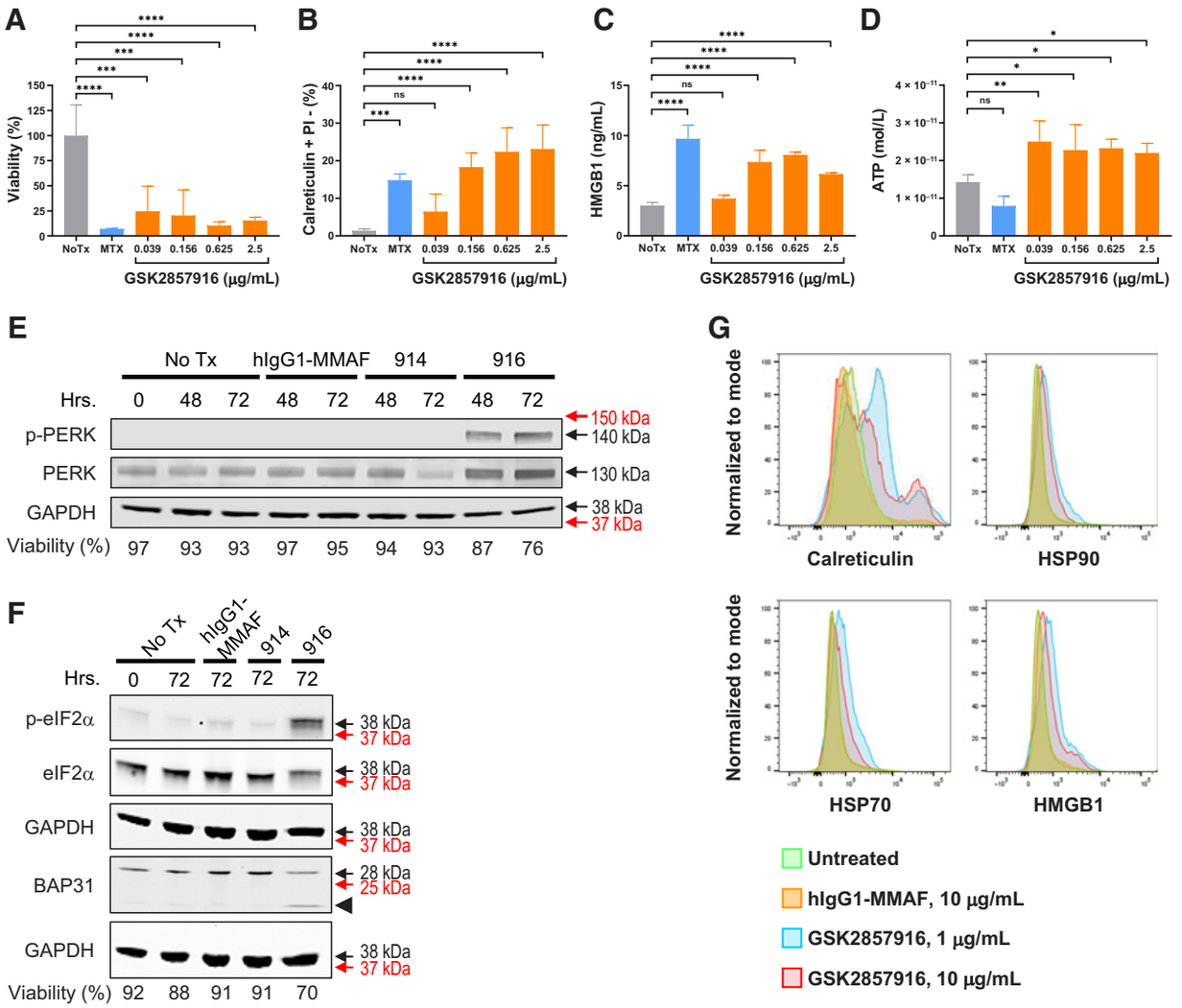

Figure 1.

GSK2857916 induces ICD markers in NCI-H929 cells. **A,** Cell viability was measured by automated flow cytometry 48 hours after treatment. **B,** Calreticulin translocation to the cell surface was assessed by flow cytometry 48 hours after treatment. Gating on PI staining allowed to exclude dead cells. **C,** HMGB1 release into the media was assessed by ELISA. **D,** Extracellular ATP concentrations in the media were determined by a luciferase-based assay. For all measurements, mean ± SD of triplicates from a representative experiment shown. A one-way ANOVA statistical analysis was performed. NCI-H929 cells were treated with 10 μg/mL (**E**) or 1 μg/mL (**F**) of hIgG1-MMAF, GSK2857914 (914) or GSK2857916 (916), or were left untreated (No Tx), for 48 or 72 hours. PERK and eIF2α phosphorylation and BAP31 cleavage were evaluated by Western blot analysis. Representative results of multiple independent experiments also indicating the cell viability (%) at the time of sample collection. Note the increase in the high molecular weight band with PERK antibody upon GSK2857916 treatment, which coincides with the PERK phosphorylation (p-PERK) antibody signal. The BAF31 cleavage product is indicated by an arrowhead. GAPDH was used as loading control. Indicated in black is the predicted molecular weight of the protein and in red the molecular weight of the protein marker. **G,** Cell surface expression of calreticulin, HSP90, HSP70, and HMGB1 by flow cytometry in NCI-H929 cells after 72 hours of treatment. Overlaid histograms of nonpermeabilized stained cells shown. Gating was performed on live cells and utilized isotype controls. (*Continued on the following page.*)

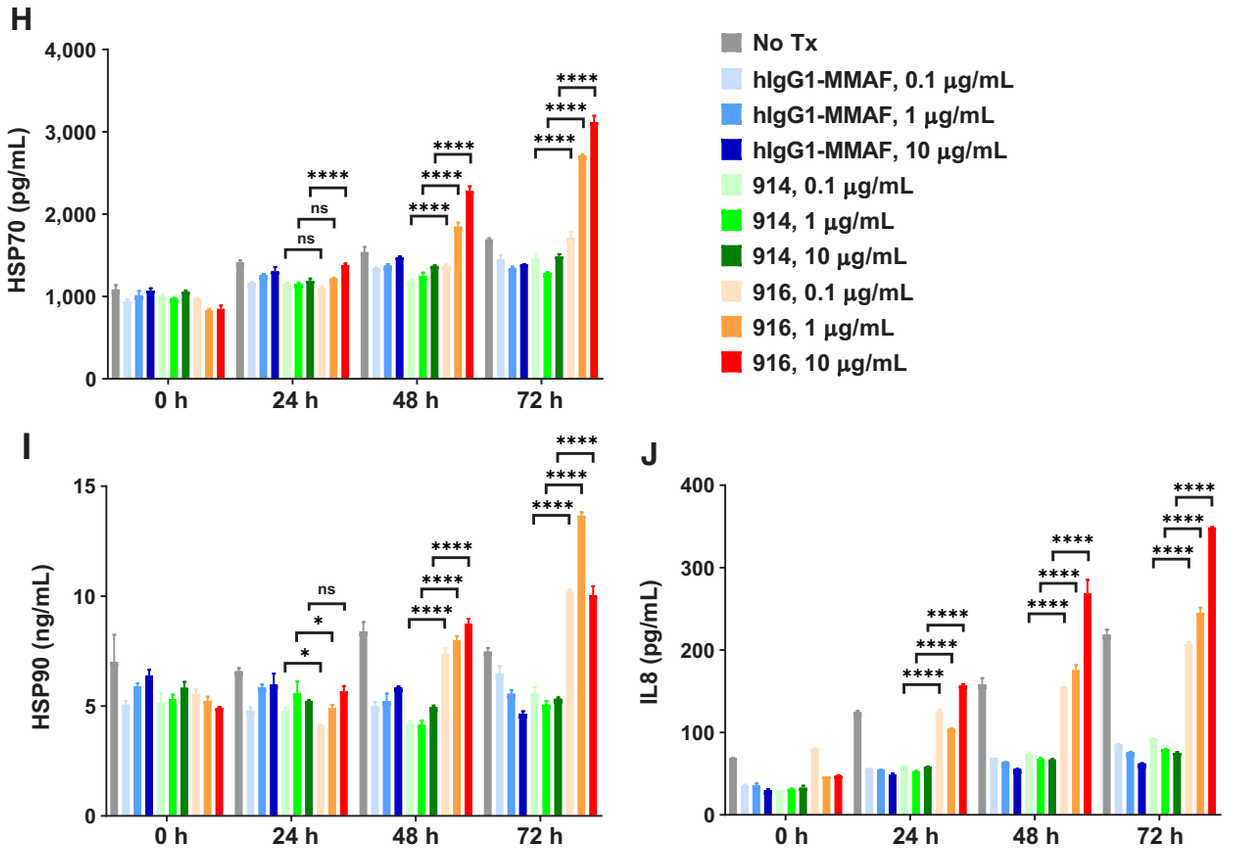

Figure 1.

(*Continued.*) **H–J,** HSP70, HSP90, and IL8 release into the media after the indicated treatments and at the indicated timepoints was assessed by ELISA in NCI-H929 cells. Shown is a representative result of at least two independent experiments, bars indicate the mean ± SD of biological duplicates. A two-way ANOVA statistical analysis was performed. ns, not significant; *, $P < 0.05$; **, $P < 0.01$; ***, $P < 0.001$; ****, $P \leq 0.0001$.

harvested 7 days after randomization and three antibody doses and fixed in 10% neutral buffered formalin, transferred to 70% ethanol and processed into paraffin blocks. IHC staining used a Ventana instrument and reagents (Ventana Medical Systems) and was performed with an anti-CD8 mAb (eBioscience; 4SM15; catalog No. 14-0808-82). Subjective histopathology assessment of hematoxylin and eosin–stained and/or IHC-stained tumor sections was completed by a board-certified veterinary pathologist.

Statistical analyses

Statistical significance was evaluated by a one-way or a two-way ANOVA using GraphPad Prism software (v8), as indicated in each figure legend, *P* values are only reported for preplanned treatment comparisons.

Ethics declarations

Fresh human blood was obtained from GlaxoSmithKline's on-site blood donation unit, and its ethical research use was in accord with the terms of the local informed consent under an Advarra Institutional Review Board–approved protocol. All animal studies were conducted in accordance with the GlaxoSmithKline Policy on the Care, Welfare and Treatment of Laboratory Animals and were reviewed and approved by the Institutional Animal Care and Use Committee either at GlaxoSmithKline or by the ethical review process at the institution where the work was performed.

Results

Induction of immunogenic cell death and DC activation by GSK2857916

Recent studies have demonstrated that microtubule-disrupting agents, such as dolastatin 10 and MMAE, can induce ICD and promote an anti-tumor response that is mediated by the adaptive immune system (22, 23, 25). Therefore, we sought to determine whether GSK2857916 induces hallmarks of ICD through induction of ER stress and autophagy and involving calreticulin cell surface exposure and release of DAMPs including ATP and HMGB1 (9, 26–30).

Treatment with GSK2857916 significantly decreased the viability of BCMA-expressing NCI-H929 human multiple myeloma cells (**Fig. 1A**) and also led to a significant and dose-dependent externalization and plasma membrane exposure of calreticulin (**Fig. 1B**) and secretion of HMGB1 and ATP into the culture media (**Fig. 1C** and **D**). Consistently, in NCI-H929 cells, GSK2857916 induced an ER stress response by promoting the phosphorylation of the ER stress kinase PERK (**Fig. 1E**) and its substrate, the eukaryotic translation initiation factor eIF2α (**Fig. 1F**), leading to the proteolytic cleavage of the ER protein B-cell receptor–associated protein (BAP) 31 (**Fig. 1F**,

arrowhead), which is critical for calreticulin exposure. Moreover, GSK2857916 treatment induced cell surface exposure (**Fig. 1G**) and significant extracellular release of other DAMPs, including HSP70 and HSP90 (**Fig. 1H** and **I**), and IL8 (**Fig. 1J**); the latter being an ICD marker indicative of immune response modulation and inflammatory response initiation. Notably, the dose- and time-dependent induction and release of these DAMPs was GSK2857916 treatment-specific and required BCMA binding and toxin release (as no changes were observed with the hIgG1-MMAF isotype or the nonconjugated GSK2857914 antibody). Furthermore, the enhanced DAMP release was observed despite decreases in cell viability (∼10%–20% less) and cell number (∼1.5- to 2-fold decrease), compared with controls (Supplementary Table S1A).

Once the ER stress response has triggered the exposure and release of calreticulin and other ER chaperones, these DAMPs act as "eat me" signals, and in concert with the chemoattractant ATP, promote the uptake of dying cells by APCs. DCs are APCs that can activate resting naïve T lymphocytes and play a key role in priming robust adaptive antitumor immune responses (31). To characterize the immune-modulatory effects of GSK2857916, we investigated the effect of GSK2857916-treated NCI-H929 tumor cells on immature DCs (iDCs) from three healthy donors. Markedly lower CD11c and HLA-DR expression on NCI-H929 cells enabled the distinction from high $CD11c^+$ and $HLA\text{-}DR^+$ DCs (**Fig. 2A**; Supplementary Fig. S1). Twenty-four hour co-culture of iDCs with GSK2857916-pretreated tumor cells led to a significant dose-dependent increase in DC activation and cell surface maturation markers including CD40, CD83, and CD86 (**Fig. 2B**). These results show that GSK2857916-induced ICD in tumor cells can modulate immune function by promoting a more active and mature DC phenotype.

Development and characterization of the EL4-hBCMA murine syngeneic model

To determine whether the *in vitro* GSK2857916-induced ICD phenotype translates into increased immunogenicity, activation of an adaptive immune response, and enhanced antitumor activity *in vivo*, an immune-competent mouse tumor model was developed. As GSK2857916 is not cross-reactive with murine BCMA, the murine EL4 T-cell lymphoma cell line was engineered to stably express hBCMA on the cell surface, at levels approaching those of the NCI-H929 multiple myeloma cells (**Fig. 3A**). GSK2857916 induced cell death in this cell line in a manner that was dependent on both the conjugated toxin and hBCMA cell surface expression (**Fig. 3B** vs. **C**). However, the EL4-hBCMA cell line was less sensitive to the cytotoxic effects of GSK2857916 as compared with NCI-H929 cells [**Fig. 3B**, mean half maximal inhibitory concentration (IC_{50}) 30.6 vs. 0.003 μg/mL, respectively]. Previous studies have shown that rodent cells are less sensitive to microtubule poisons relative to primate cells (32). Consistently, the EL4 parental and EL4-hBCMA cells were also less sensitive to microtubule polymerization inhibitors including free MMAE, a cell permeable auristatin derivative similar to MMAF, vinorelbine and colchicine (Supplementary Fig. S2A–S2C). These results indicate that EL4-hBCMA cells are less sensitive to GSK2857916 compared with NCI-H929 cells, likely due to lower BCMA surface expression levels and lower intrinsic sensitivity to the cytotoxic effects of MMAF.

To evaluate whether expression of hBCMA leads to specific induction of ICD by GSK2857916, ICD markers were assessed in EL4-hBCMA cells compared with EL4 parental cells. GSK2857916 treatment of EL4-hBCMA cells (**Fig. 3D**), but not the hIgG1-MMAF or GSK2857914 controls (**Fig. 3E**), led to a dose- and time-dependent cell surface exposure of murine calreticulin. GSK2857916 had no effect on the parental EL4 cells lacking hBCMA (**Fig. 3F** vs. **G**). GSK2857916 treatment also induced surface exposure of other prominent hallmarks of ICD: HSP90, HSP70, and HMGB1 (Supplementary Fig. S2D). Furthermore, GSK2857916 treatment (at 10 and 100 μg/mL) led to significantly increased release of calreticulin, HMGB1, and HSP60 into the culture medium over time in EL4-hBCMA (**Fig. 3H**) but not EL4 parental cells (**Fig. 3I**). The significant release of DAMPs in EL4 cells was only seen at the highest dose of 100 μg/mL, presumably due to off-target MMAF cytotoxicity (33). Furthermore, the induction of ICD markers in GSK2857916-treated cells occurred despite reduced viability (∼10%–15% reduction) and cell number (∼1.7- to 2.8-fold reduction; Supplementary Table S1B vs. S1C).

Sustained antitumor activity of GSK2857916 is mediated by host innate and adaptive immune responses

Having established a murine cell line in which ICD is specifically induced by GSK2857916, we evaluated the antitumor activity of GSK2857916 against EL4-hBCMA tumors established in immune-competent mice. Tumor-bearing mice were treated with GSK2857916 doses ranging from 0.001–30 mg/kg. Dose-dependent antitumor activity, characterized by decreased tumor burden and significantly increased survival, was observed starting at 0.1 mg/kg of GSK2857916 compared with hIgG1-MMAF control ($P < 0.05$). In addition, higher doses of GSK2857916 led to significant tumor regressions, complete responses in up to 90% of tumor-bearing mice at the highest dose of 30 mg/kg, and significant long-term survival of ≥60 days (**Fig. 4A**; Supplementary Fig. S3A).

To assess whether tumor regression was associated with the establishment of an adaptive immune response, rechallenge experiments were conducted. Tumor-free surviving mice from the dose-escalation study were rechallenged with either parental EL4 or EL4-hBCMA cells on day 77 (**Fig. 4B**, green triangles vs. red diamonds, respectively). Efficacy was compared against naïve age-matched animals challenged with EL4 parental or EL4-hBCMA cells (**Fig. 4B**, black squares vs. blue triangles, respectively). All tumor-free mice that exhibited a complete response to GSK2857916 treatment rejected the rechallenge with both EL4-hBCMA and EL4 parental cells, with no new tumors developing up to 50 days after the secondary inoculation (**Fig. 4B**; Supplementary Fig. S3B). In contrast, all but one naïve animal established new tumors and ultimately succumbed to this challenge (**Fig. 4B**; Supplementary Fig. S3B). The differences between GSK2857916-exposed and naïve mice (re)-challenged with EL4 or EL4-hBCMA cells were significant ($P < 0.001$). Rejection of the parental EL4 cell line by the GSK2857916-responding animals suggests that the adaptive immune response against tumors is not directed solely at hBCMA but may target additional neo-epitopes presented by the APCs in this model.

To determine the contributions of the different mechanisms of GSK2857916 *in vivo* activity in the EL4-hBCMA syngeneic model, we examined each mechanism in isolation by comparing several versions of the GSK2857914 antibody and the GSK2857916 ADC (at the 30 mg/kg dose). The unconjugated afucosylated (Fc-enhanced) GSK2857914 antibody showed significantly decreased tumor burden (Supplementary Fig. S3C) and survival advantage (**Fig. 4C**) over the matched afucosylated hIgG1 control antibody ("hIgG1"; $P < 0.001$ and $P < 0.001$, respectively) and the fucosylated (Fc-disabled) GSK2857914 antibody ("GSK2857914 disabled;" $P < 0.001$ and $P = 0.033$, respectively). This suggests a significant contribution of the ADCC mechanism of action to *in vivo* antitumor activity. No significant differences in efficacy were observed between GSK2857914 and a GSK2857914 mouse IgG2a chimeric antibody ($P > 0.05$); the latter being the mouse

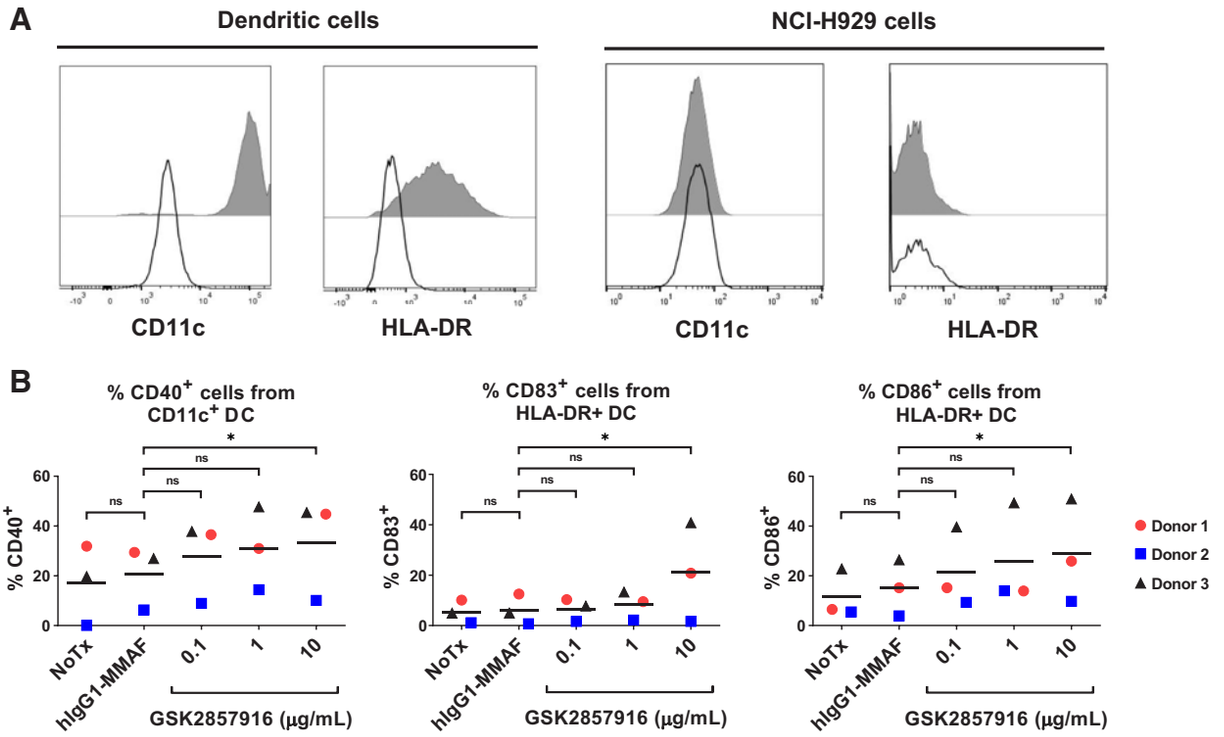

Figure 2.

GSK2857916 induces DC activation and maturation *in vitro*. Differential expression of CD11c and HLA-DR allows for a gating strategy that distinguishes isolated iDCs from NCI-H929 tumor cells. **A,** Histograms representing CD11c and HLA-DR surface expression in untreated iDCs and NCI-H929 cells. Gray, antibody histogram; white, isotype histogram. **B,** CD40, CD83, and CD86 surface expression by flow cytometry in isolated iDCs from three healthy donors following a 24-hour co-culture with NCI-H929 cells, which were pretreated as indicated for 48 hours. Shown are the percentage of positive cells per donor and mean. A two-way ANOVA statistical analysis was performed. ns, not significant; *, $P < 0.05$.

(IgG2a) functional equivalent to human IgG1. GSK2857916 treatment led to both significantly decreased tumor burden ($P < 0.001$) and increased survival ($P = 0.031$), compared with the hIgG1-MMAF control, and 40% durable complete responses (**Fig. 4C**; Supplementary Fig. S3C). We observed slightly decreased tumor burden ($P = 0.979$) and increased survival ($P < 0.001$) after hIgG1-MMAF treatment compared with saline control, at 30 mg/kg (**Fig. 4C**; Supplementary Fig. S3C) but not 10 mg/kg (Supplementary Fig. S3A). Previous studies have shown off-target cytotoxicity of ADCs by premature release of cytotoxic drug or uptake of intact ADCs by both receptor-dependent (FcγRs, FcRn, and C-type lectin receptors) and receptor-independent (pinocytosis, macropinocytosis) mechanisms (33). Such off-target mechanisms, particularly macropinocytosis, have been proposed to explain the ocular findings observed in patients treated with GSK2857916 (34) and other ADCs (35). Notably, neither complete regressions nor tumor-free animals were observed after treatment with the unconjugated antibodies (Supplementary Fig. S3C). Because in this mouse model, complete regressions and resistance to rechallenge were only obtained with GSK2857916, durable antitumor responses must require MMAF-induced ICD and an adaptive immune response.

To further examine the contribution of GSK2857916 to an adaptive immune response, we performed transient lymphodepletion studies using specific CD4 and CD8 antibodies in GSK2857916 or hIgG1-MMAF treated animals (15 mg/kg; **Fig. 5A–J**). Depletion of $CD4^+$ and $CD8^+$ T cells was confirmed by flow cytometry on day 15 post-treatment (**Fig. 5I** and **J**). Depletion of $CD8^+$ T cells completely abrogated GSK2857916-mediated antitumor activity and complete tumor regressions (**Fig. 5E** vs. **G**, $P = 0.001$; Supplementary Fig. S4). In contrast, depletion of $CD4^+$ T cells did not significantly alter GSK2857916-mediated antitumor activity (**Fig. 5E** vs. **F**, $P = 0.98$; Supplementary Fig. S4). The combined depletion of $CD4^+$ and $CD8^+$ T-cell populations did not significantly enhance the effects observed by the single $CD8^+$ T-cell depletion (**Fig. 5G** vs. **H**, $P = 0.98$; Supplementary Fig. S4), further supporting a preponderant role for $CD8^+$ T cells in mediating antitumor activity in this model. We observed a slight growth delay in GSK2857916, $CD8^-$ animals (**Fig. 5G** and **H** vs. **C** and **D**; Supplementary Fig. S4) potentially attributable to ADCC.

Collectively, these results support the hypothesis that GSK2857916 promotes the development of an adaptive tumor-specific immune response, in addition to its previously reported innate immune activity, and highlight the immunogenic potential of GSK2857916 along with GSK2857916-mediated tumor antigen spreading.

GSK2857916 enhances intratumor immune cell infiltration and activation

The pharmacodynamic effects of GSK2857916 were assessed *in vivo* using the EL4-hBCMA immune-competent model. In the absence of treatment, BCMA expression in this mouse model was maintained on EL4-hBCMA tumor cells (Supplementary Fig. S5A), while there was a significant reduction in dendritic (CD11c) and natural killer (NK;

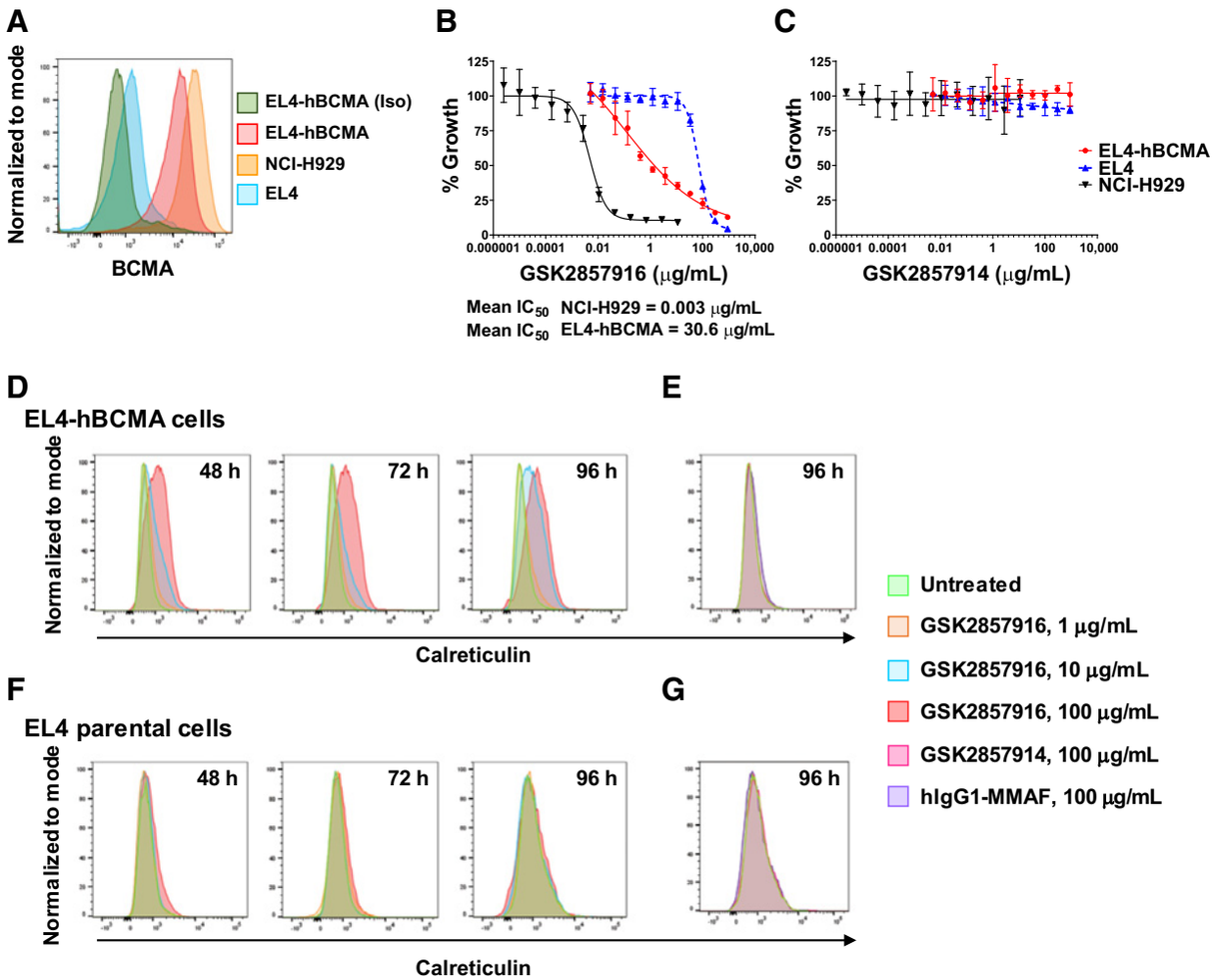

Figure 3.

GSK2857916 induces ICD markers in EL4-hBCMA cells. **A,** BCMA cell surface expression by flow cytometry in EL4-hBCMA, EL4 parental, and NCI-H929 cells. Overlaid histograms depicting BCMA normalized median fluorescence intensity (MFI) in nonpermeabilized stained cells shown. Gating was performed on live cells and utilized isotype controls. Dose–response curves in EL4-hBCMA, EL4 parental, and NCI-H929 cells, following 3 days of exposure to GSK2857916 (**B**) or GSK2857914 (**C**). Shown is representative data normalized to % growth from at least three independent experiments with mean ± SD of biological quadruplicates. Mean IC_{50} values from at least three independent experiments also reported. **D,** Calreticulin cell surface expression by flow cytometry in EL4-hBCMA cells at the indicated timepoints in untreated cells and after exposure to 1, 10, or 100 μg/mL of GSK2857916 *in vitro*. Overlaid histograms of nonpermeabilized stained cells shown. Gating was performed on live cells and utilized isotype controls. **E,** Calreticulin cell surface expression as in (**D**) 96 hours after exposure to 100 μg/mL of GSK2857914 or hIgG1-MMAF and in untreated cells *in vitro*. **F** and **G,** Calreticulin cell surface expression as in (**D** or **E**) in EL4 parental cells. (*Continued on the following page.*)

CD49b) cell infiltration during tumor development and progression (Supplementary Fig. S5B).

Furthermore, changes in pharmacodynamic markers *in vivo* following treatment with GSK2857916 were also assessed 24 hours after a second dose of GSK2857916 (15 mg/kg). Immunophenotyping of the tumors by flow cytometry revealed a significant increase in infiltrating $CD8^+$ T cells after GSK2857916 treatment (**Fig. 6A**); which exhibited significantly increased activation markers including CD25, CD69, and inducible T-cell costimulator (ICOS; **Fig. 6B**). We also observed a significant increase in both $CD8^+PD\text{-}1^+$ cells (**Fig. 6B**) and $CD8^+$ granzyme B (GrzB)+ cytotoxic cells (**Fig. 6C**). GSK2857916 treatment also significantly increased $CD4^+$ T-cell infiltration (**Fig. 6A**) and proliferation; and resulted in a significant increase in regulatory T cells (Treg: $CD4^+CD25^+FoxP3^+$; **Fig. 6A**) in the tumor, only when compared with saline. Increase in tumor-infiltrating Tregs has been reported with other ADCs (23) and did not seem to interfere with GSK2857916 antitumor effects. Moreover, upregulation of Tregs in the tumor microenvironment has been proposed to control autoreactive effector T cells and prevent autoimmunity and adverse events (23, 36, 37). GSK2857916 also significantly increased NK cell ($CD49^+$; **Fig. 6C**) and DC infiltration ($CD11c^+$; **Fig. 6A**), and expression of the costimulatory molecule CD86 (**Fig. 6C**), indicating increased DC activation. An independent experiment evaluating TILs by IHC 7 days after treatment onset confirmed GSK2857916-dependent increases in infiltrating $CD8^+$ T cells (**Fig. 6D**; Supplementary Fig. S5C). Moreover, consistent with ICD induction, GSK2857916 treatment led to a reproducible increase in calreticulin expression on the surface of hBCMA-expressing tumor cells *in vivo* (**Fig. 6E**). *In vivo*

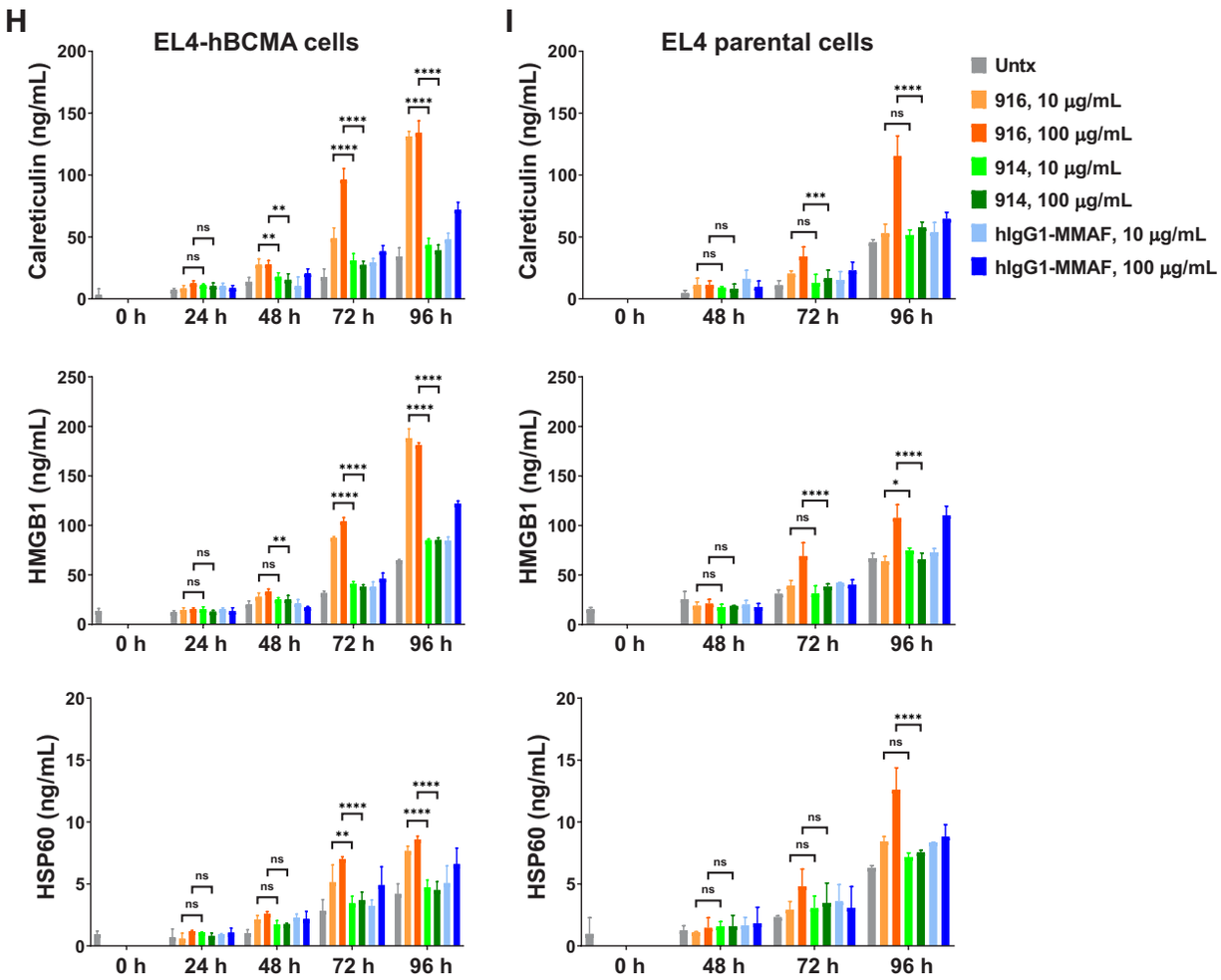

Figure 3.

(*Continued.*) Calreticulin, HMGB1 and HSP60 release into the media after the indicated treatments and at the indicated timepoints assessed by ELISA in EL4-hBCMA (**H**) and EL4 parental (**I**) cells. Shown is a representative result of at least two independent experiments, bars indicate the mean ± SD of biological duplicates or triplicates. A two-way ANOVA statistical analysis was performed. ns, not significant; *, $P < 0.05$; **, $P < 0.01$; ***, $P < 0.001$; ****, $P \leq 0.0001$.

ICD was further supported by gene expression analysis of tumors by NanoString, where GSK2857916 treatment induced the expression of a type I IFN-related gene signature (**Fig. 6F**; ref. 24).

Combining GSK2857916 with an agonist anti-OX86 antibody increases *in vivo* efficacy

GSK2857916 induced ICD and intratumoral immune cell infiltration and activation *in vivo*, and increased expression of the costimulatory molecule OX40 in $CD8^+$ and $CD4^+$ infiltrating T cells (Supplementary Fig. S5D). We therefore hypothesized that GSK2857916 may synergize with immune-modulatory agents. We evaluated combinations with OX86, a mouse anti-OX40 IgG2a mAb, with a suboptimal dose of GSK2857916 (10 mg/kg) in the EL4-hBCMA syngeneic model. Combining GSK2857916 with OX86 at 0.2, 1, and 5 mg/kg provided additional benefit compared with each single agent by significantly decreasing tumor burden ($P \leq 0.002$) and increasing survival ($P \leq 0.003$; **Fig. 7**; Supplementary Fig. S6A–S6C), and resulted in 70%, 40%, and 50% tumor-free mice, at the respective OX86 doses, at the end of the study (day 60; Supplementary Fig. S6B). In contrast, there were no tumor-free mice in the groups treated with GSK2857916 or 0.2 mg/kg OX86 alone, and only one tumor-free mouse in each of the groups receiving 1 or 5 mg/kg OX86 alone (Supplementary Fig. S6A and S6B). Further confirming the role of effector T cells in GSK2857916-mediated antitumor activity and immunologic memory, all tumor-free mice at end of study were immune to rechallenge with EL4-hBCMA cells in an independent experiment.

Discussion

Over the last decade, the 5-year survival rates for patients with multiple myeloma have increased to approximately 50%, fueled by several new regulatory approvals (38). A wide array of treatment options are now available to patients including autologous stem cell transplant, proteasome inhibitors (bortezomib and carfilzomib), and immune-modulatory agents (thalidomide, lenalidomide, and pomalidomide). More recently, additional agents with novel mechanisms of action have been developed like panobinostat, a histone deacetylase

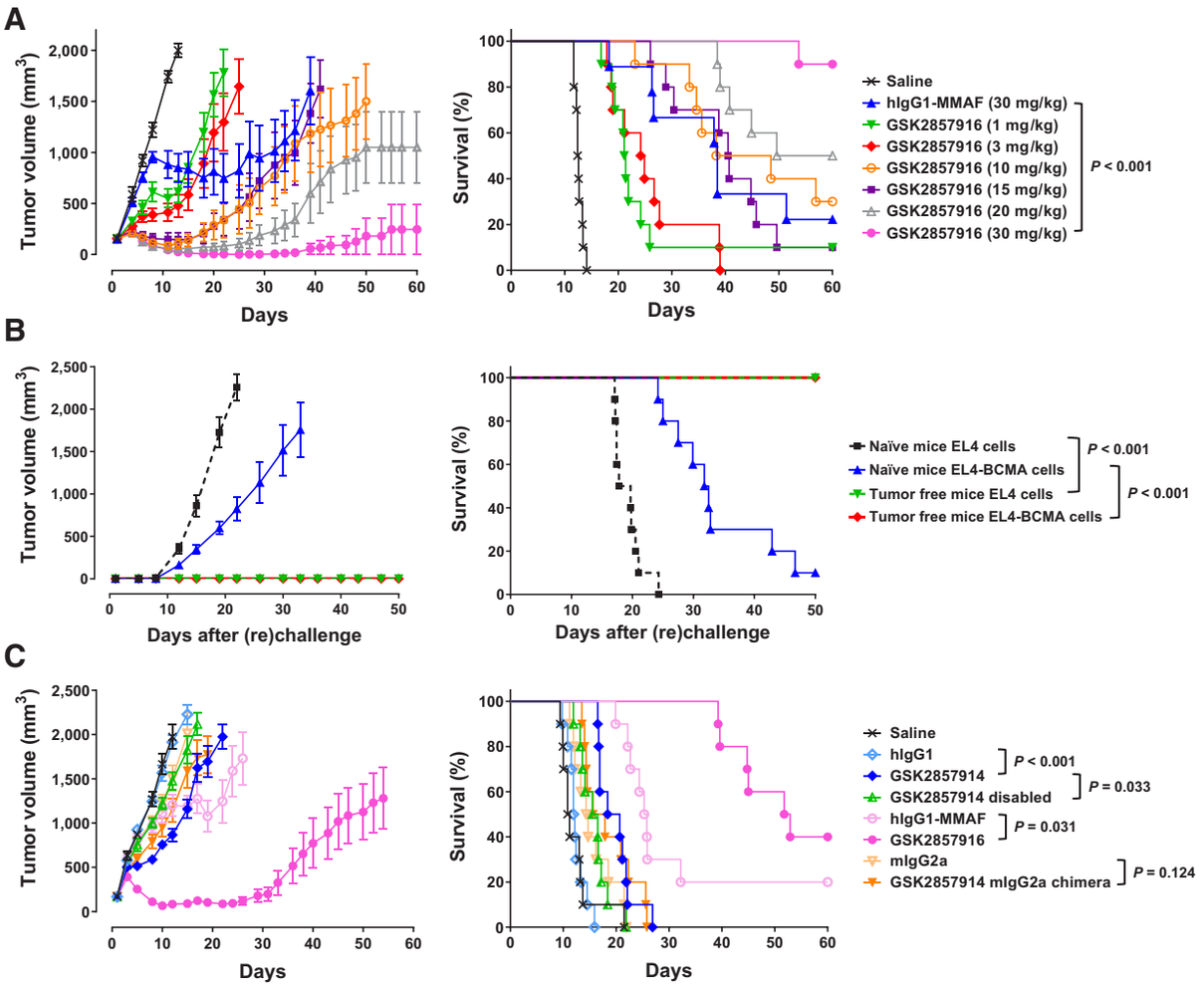

Figure 4.

GSK2857916 *in vivo* antitumor activity is mediated by host innate and adaptive immune responses and is MMAF dependent. **A,** Therapeutic efficacy (left) and survival (right) in C57BL/6 mice bearing EL4-hBCMA tumors. Animals were treated intraperitoneally when tumors reached approximately 150 to 200 mm^3 with saline, hIgG1-MMAF or increasing doses of GSK2857916 twice a week for 3 weeks, as indicated ($n = 10$ mice/group). **B,** Animals with complete and sustained tumor regressions from (**A**; $n = 9$ mice/group) and age-matched naïve controls ($n = 10$ mice/group) were (re)-challenged with 1×10^5 EL4-hBCMA or EL4 parental cells on day 77 (the last dose of GSK2857916 was on day 17). Therapeutic efficacy (left) and survival (right) were monitored for 50 days after cell (re)-inoculation. **C,** Therapeutic efficacy (left) and survival (right) in EL4-hBCMA tumor-bearing mice dosed with 30 mg/kg as in (**A**) with several versions of the GSK2857914 antibody or the GSK2857916 ADC, as indicated ($n = 10$ mice/group). Efficacy data expressed as mean tumor volume ± SEM, over time. Kaplan–Meier survival in percentage, significant *P* values by a standard log-rank test ($P < 0.05$).

inhibitor, and selinexor, a selective inhibitor of the nuclear export protein XPO1. Furthermore, mAbs targeting cell surface receptors such as CD38 (daratumumab, isatuximab) and CD319/CS1/signaling lymphocyte activation molecule family (SLAMF) 7 (elotuzumab) have shown anti-neoplastic effects on malignant plasma cells by coopting the innate immune system and eliciting NK cell–mediated ADCC. However, the immune system of patients with multiple myeloma is often significantly compromised contributing to tumor cell immune evasion and suppression (39). Therefore, therapeutic approaches aimed at inducing adaptive immune responses that potentiate tumor-specific immunity represent an exciting area in the treatment of multiple myeloma.

GSK2857916 was evaluated in phase I and II studies in patients with relapsed/refractory multiple myeloma (RRMM) and other hematologic malignancies (NCT02064387 and NCT03525678, respectively; www.clinicaltrials.gov), demonstrating clinically meaningful efficacy with a manageable safety profile in patients with RRMM (40–42). Furthermore, the FDA and the European Commission recently approved BLENREP (GSK2857916, belantamab mafodotin) as a first-in-class, BCMA targeting therapy for adult patients with RRMM, who have received at least four prior therapies. These clinical studies were supported by the nonclinical evidence that GSK2857916 inhibits tumor growth and prolongs survival in disseminated SCID mouse models bearing human multiple myeloma xenografts (20). The antitumor activity of GSK2857916 was attributed to the direct effect of the toxin (MMAF) on proliferating tumor cells and to NK cell–mediated and macrophage-mediated ADCC and ADCP, respectively. To allow for the engraftment of human tumor cells, the mice used in the previous nonclinical studies did not contain functional T or B cells and consequently, the secondary effects of adaptive tumor immunity

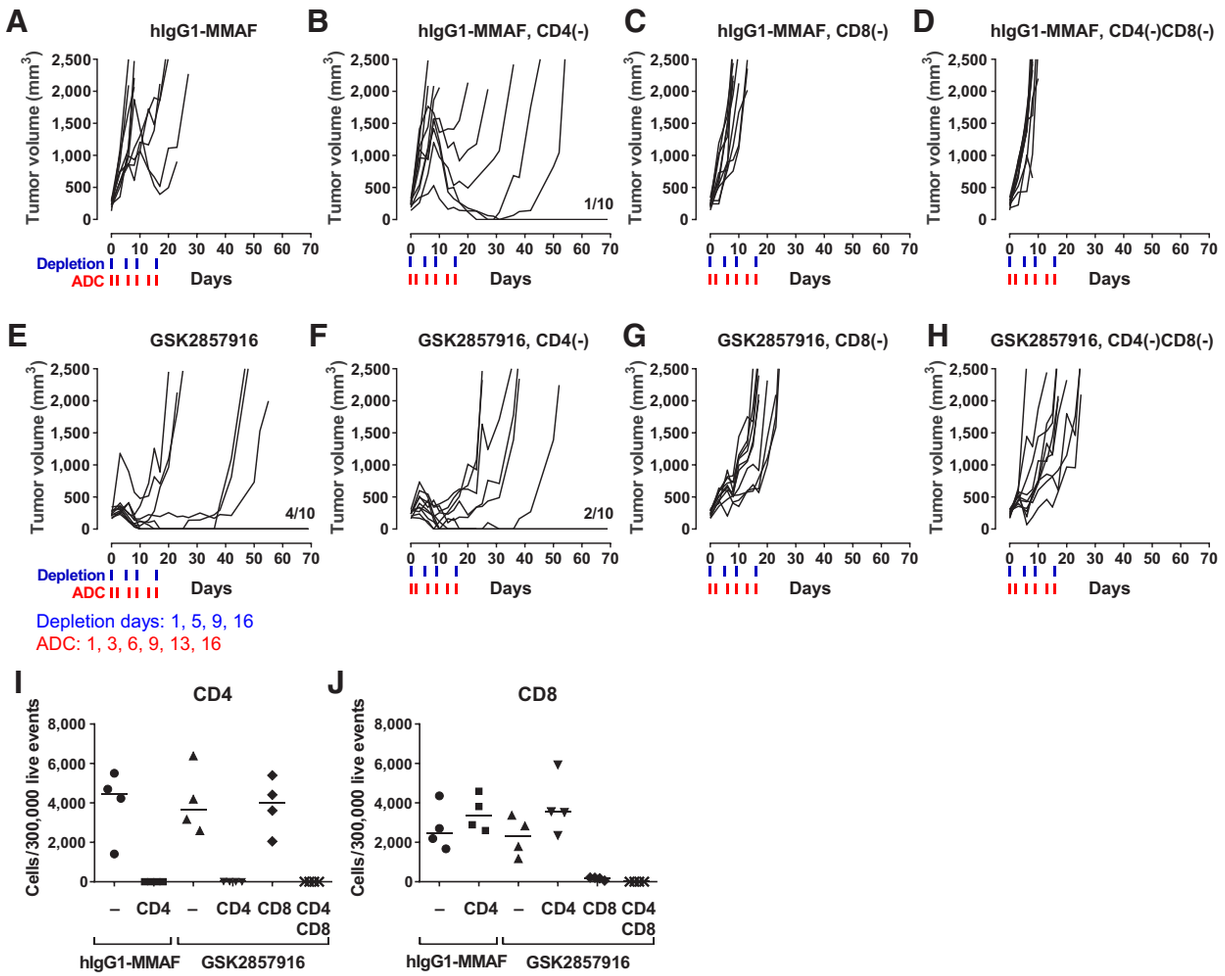

Figure 5.

Depletion of CD8$^+$ T cells abrogates GSK2857916 antitumor activity. **A–H,** EL4-hBCMA tumors were established (as in **Fig. 4**) and animals were treated on days 1, 3, 6, 9, 13, and 16 with GSK2857916 or hIgG1-MMAF (15 mg/kg; red ticks labeled as "ADC"). T-cell–depleting doses of anti-CD4, anti-CD8, or both (300 μg/mouse) were administered on days 1, 5, 9, and 16 (blue ticks labeled as "Depletion"). Efficacy data expressed as individual tumor volumes over time ($n = 10$ mice/group). The number of tumor free/total mice is indicated in the bottom right corner. **I** and **J,** Depletion of CD4$^+$ and/or CD8$^+$ T cells was verified on day 15 by flow cytometry.

were not explored or accounted for in the initial characterization of GSK2857916 mechanism of action in these mouse models.

Microtubule-disrupting agents belonging to the maytansine and auristatin family of cytotoxic agents (22, 25) and ADCs bearing pyrrolobenzodiazepines or tubulysin (Tub) payloads (43), have recently been shown to promote functional DC maturation and activation, and greater antitumor activity in immune-competent versus immune-deficient mice. Brentuximab vedotin (an anti-CD30 antibody linked to the payload MMAE) and trastuzumab emtansine (an anti-HER2 antibody linked to the maytansine derivative DM1) are approved ADCs with clinical activity in patients with cancer, shown to promote DC maturation resulting in T-cell priming and adaptive immune responses (22, 23). In this study, we provide evidence that GSK2857916 elicits similar immune effects and antitumor responses. Our *in vitro* studies with human and mouse tumor cell lines are the first to demonstrate that GSK2857916 induces an ER stress response that ultimately leads to the production of DAMPs (including calreticulin, HMGB1, ATP) and primes an ICD response in tumor cells in a manner that is dependent on MMAF and BCMA cell surface expression. Furthermore, exposure of human primary immature DCs to tumor cells undergoing GSK2857916-mediated ICD results in DC maturation and activation. DCs represent a rare but key immune cell subset central to developing innate and adaptive immune responses, and much interest exists in modulating their function for the betterment of cancer immunotherapies (44). Our results are in line with prior reports in which the ability of cells to undergo immunogenic apoptosis relied on calreticulin exposure to enable the engulfment of dying tumor cells by DCs (45). Furthermore, exposure or release of other DAMPs including HSP70, HSP90, and ATP, may further enhance DC migration and activation, and cross-presentation of tumor antigens to CD8$^+$ CTLs (46). Interestingly, HSPs are also able to interact with and activate NK cells (47), which might further enhance GSK2857916 antitumor activity. In this way, ICD offers additional benefits by boosting the host immune system through tumor-specific immunity.

As described, ICD is believed to stimulate immune responses subsequent to the recognition of dying tumor cells by DCs and tumor antigen presentation. Engagement of the immune system in this manner can lead to complete tumor regression and long-term adaptive

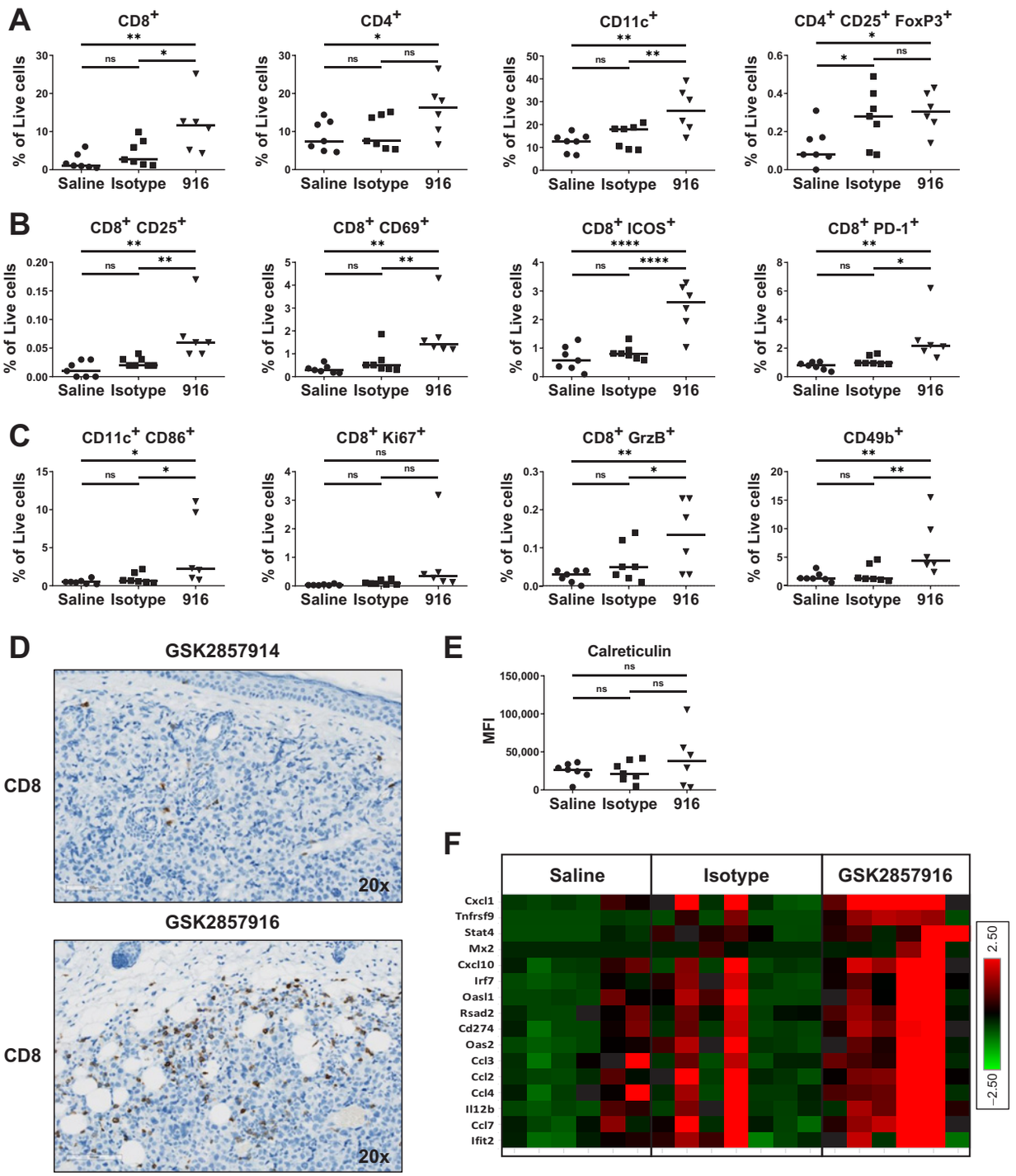

Figure 6.

GSK2857916 enhances intratumor immune cell infiltration and activation. Quantification by flow cytometry of immune cells infiltrating C57BL/6 mice bearing EL4-hBCMA tumors following treatment with GSK2857916 or isotype control (at 15 mg/kg), or saline vehicle. **A,** $CD8^+$, $CD4^+$, and regulatory ($CD4^+CD25^+FoxP3^+$) T cells, and DC ($CD11c^+$). **B,** T-cell activation markers CD25, CD69, and ICOS and the exhaustion marker PD-1. **C,** Quantification of the DC costimulatory molecule CD86, T-cell proliferation (Ki67) and cytotoxicity (granzyme B, GrzB) in TILs and NK cells ($CD49b^+$). A one-way ANOVA statistical analysis was performed. ns, not significant; *, $P < 0.05$; **, $P < 0.01$; ***, $P < 0.001$; ****, $P \leq 0.0001$. **D,** IHC for CD8 reactive cells in mice bearing EL4-hBCMA tumors treated with GSK2857914 (top) or GSK2857916 (bottom) at 15 mg/kg (as in **Fig. 4**). Representative images, 20× magnification. **E,** Quantification of calreticulin cell surface expression (MFI) on tumor cells in mice. **F,** Heatmap depicting a type I IFN-related gene signature following treatment with saline, isotype control or GSK2857916 (at 15 mg/kg) from the same experiment as in **(A–C**, **E)**. Each column represents an individual mouse and each row an individual gene.

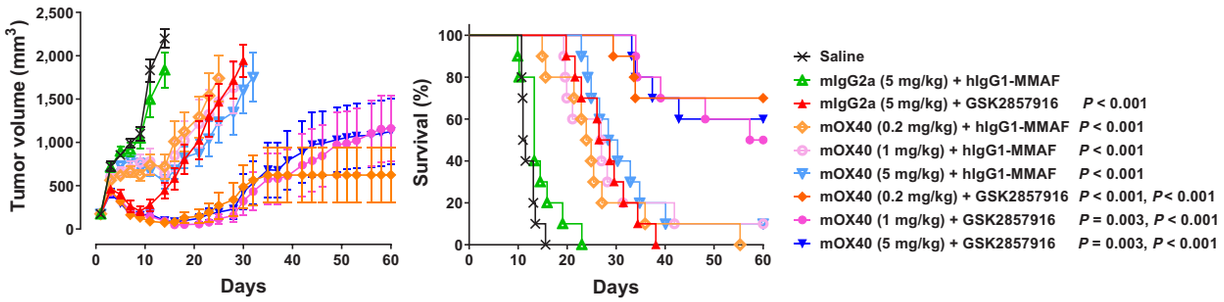

Figure 7.

Therapeutic synergy by combining GSK2857916 and an agonist anti-OX86 antibody. Therapeutic efficacy (left) and survival (right) in C57BL/6 mice bearing EL4-hBCMA tumors. Animals were treated intraperitoneally when tumors reached approximately 150 to 200 mm^3 with GSK2857916 or hIgG1-MMAF at 10 mg/kg and/or a mouse anti-OX86 IgG2a or IgG2a isotype antibody at 0.2, 1, and 5 mg/kg, plus saline control, all twice a week for 3 weeks, as indicated. Efficacy data expressed as mean tumor volume ± SEM over time. Kaplan–Meier survival in percentage, significant *P* values by a standard log-rank test ($P < 0.05$; $n = 10$ mice/group) provided for the combination against the first or second single agent listed, respectively.

immunity against the inoculated cancer cells. Furthermore, tumor cells succumbing in a manner that is immunogenic can elicit a protective response against a subsequent challenge with live tumor cells (48). Indeed, GSK2857916 treatment of immune-competent mice bearing syngeneic EL4-hBCMA tumors resulted in potent antitumor activity and robust activation of adaptive immune responses, which included intratumor dendritic, NK- and T-cell infiltration and activation, and maturation of immune cell subsets. These immune responses were likely enhanced by the GSK2857916-dependent induced expression of type I IFN gene signatures, which are known to elicit chemotherapy-dependent antitumor immunity by several mechanisms including promoting cross-priming, supporting CTLs and immune effector functions, and releasing proinflammatory cytokines. Intratumoral expression of such gene signatures has been correlated with favorable disease outcomes in patients with cancer (24, 49). Importantly, $CD8^+$ T cells were indispensable for the potent and durable GSK2857916 antitumor activity in our immune-competent mouse model. The requirement for $CD8^+$, but not $CD4^+$, T cells was previously reported for other ADCs such as dolastatins (22), pyrrolobenzodiazepines, and Tub (43), and underlines the importance of DCs and subsequently T cells for the full therapeutic potential of ADCs and of GSK2857916. Notably, the GSK2857916 cytotoxic payload, MMAF, is non-cell permeable, suggesting that ICD and subsequent DC responses are likely mediated by the BCMA-expressing EL4 tumor cells and not as a result of bystander effects on neighboring "non-target" cells. Furthermore, the capacity of immune-competent mice to reject a rechallenge with EL4 parental or EL4-hBCMA tumor cells after surviving the initial inoculation, supports the role of the immune system in protecting against cancer cells and the idea of tumor-specific antigen spreading and immunologic memory; revealing a novel mechanism of action for GSK2857916. Recent nonclinical studies showed that therapeutic approaches that induce ICD, activate DCs, and promote the priming of tumor antigen-specific T cells can sensitize to immune checkpoint therapy (50). Concordantly, our *in vivo* combination results suggest that the antitumor activity of GSK2857916 may be further enhanced through combinations with T-cell immune checkpoint inhibitors.

Finally, GSK2857916 multiple mechanisms of action provide advantages over other multiple myeloma therapies. First, the targeted cytotoxic ADC activity of GSK2857916 offers a unique advantage over other "ADCC only" agents in multiple myeloma. Second, the ADCC/ADCP effector activity of GSK2857916 also contributes to the compound's antitumor activity. The enhanced ADCC activity mediated by the afucosylated Fc portion of GSK2857916 may target multiple mediators of the host immune response resulting in potential synergistic antitumor immunity via induction of both innate and adaptive immune pathways. Third, GSK2857916 enhanced antigen presentation through ICD and resulting T-cell–mediated durable immunity may provide added therapeutic benefit alone or in combination with immune-enhancing agents. Clinically, there is broad interest in combining immune checkpoint modulation with agents that may increase tumor immunogenicity, potentially expanding the proportion of patients that respond to therapy and favoring achieving minimal residual disease.

Here, we describe a novel immune-based mechanism of action for GSK2857916 and its potential for combining with immune-therapeutic agents, providing rationale for testing such combinations in clinical trials; some being evaluated as part of the DREAMM (DRiving Excellence in Approaches to Multiple Myeloma) clinical trial program.

Authors' Disclosures

R. Montes de Oca reports other support from GlaxoSmithKline outside the submitted work. D.C. Cooper reports other support from GlaxoSmithKline outside the submitted work. H. Jackson reports personal fees from GlaxoSmithKline during the conduct of the study and personal fees from GlaxoSmithKline outside the submitted work. O. Kepp reports other support from GlaxoSmithKline during the conduct of the study. A. Sauvat reports grants from GlaxoSmithKline during the conduct of the study. G. Kroemer reports grants from GlaxoSmithKline during the conduct of the study; grants from Bayer Healthcare, Daiichi Sankyo, Kaleido, Lytix Pharma, PharmaMar, Samsara, Sanofi, Sotio, Vascage, Vasculox/Tioma, and Elior outside the submitted work; in addition, G. Kroemer has a patent for Compounds regulating calreticulin, KDEL receptor and/or Erp-57 cell surface exposure and uses thereof to evaluate the efficiency of a cancer treatment issued, a patent for Inhibitors of protein phosphatase 1, GADD34 and protein phosphatase 1/GADD34 complex, preparation and uses thereof pending, a patent for Kits and methods for detecting the ability to induce an immunogenic cancer cell death in a subject pending, a patent for Calreticulin for its use as a medication for the treatment of cancer in a mammal pending, and a patent for Compounds and uses thereof to induce an immunogenic cancer cell death pending; and G. Kroemer is on the Board of Directors of the Bristol Myers Squibb Foundation. G. Kroemer is a scientific cofounder of EverImmune, Samsara Therapeutics, and Therafast Bio. C. Shelton reports personal fees from GlaxoSmithKline during the conduct of the study and personal fees from GlaxoSmithKline outside the submitted work. P. Mayes reports other support from GlaxoSmithKline outside the submitted work; in addition, P. Mayes has a patent for Combination treatments and uses and methods thereof pending. J. Opalinska reports other support from GlaxoSmithKline and other support from GlaxoSmithKline outside the submitted

work; in addition, J. Opalinska has a patent for Combinations with Belamaf pending; and stock ownership, employment. No disclosures were reported by the other authors.

Authors' Contributions

R. Montes de Oca: Conceptualization, resources, data curation, formal analysis, supervision, validation, investigation, visualization, methodology, writing–original draft, project administration, writing–review and editing. **A.S. Alavi:** Conceptualization, data curation, formal analysis, supervision, investigation, visualization, methodology, writing–original draft, writing–review and editing. **N. Vitali:** Formal analysis, investigation, methodology. **S. Bhattacharya:** Conceptualization, formal analysis, investigation, methodology, writing–review and editing. **C. Blackwell:** Conceptualization, formal analysis, investigation, methodology, writing–review and editing. **K. Patel:** Conceptualization, formal analysis, investigation, methodology, writing–review and editing. **L. Seestaller-Wehr:** Conceptualization, formal analysis, investigation, methodology, writing–review and editing. **H. Kaczynski:** Formal analysis, investigation, methodology. **H. Shi:** formal analysis, investigation, methodology, writing–review and editing. **E. Dobrzynski:** Investigation, methodology, writing–review and editing. **L. Obert:** Formal analysis, investigation. **L. Tsvetkov:** Conceptualization, formal analysis, investigation. **D.C. Cooper:** Formal analysis, writing–review and editing. **H. Jackson:** Formal analysis, writing–review and editing. **P. Bojczuk:** Investigation, methodology. **S. Forveille:** Investigation, methodology. **O. Kepp:** Conceptualization, formal analysis, supervision, methodology, writing–review and editing. **A. Sauvat:** Investigation, methodology. **G. Kroemer:** Conceptualization, resources, funding acquisition, writing–review and editing. **M. Creighton-Gutteridge:** Methodology. **J. Yang:** Conceptualization, supervision. **C. Hopson:** Resources, supervision. **N. Yanamandra:** Resources, supervision. **C. Shelton:** Resources, formal analysis, writing–review and editing. **P. Mayes:** Conceptualization, supervision. **J. Opalinska:** Funding acquisition, writing–review and editing. **M. Barnette:** Resources, funding acquisition. **R. Srinivasan:** Resources, funding acquisition. **J. Smothers:** Resources, funding acquisition. **A. Hoos:** Resources, funding acquisition.

Acknowledgments

The study was funded by GlaxoSmithKline Oncology Research & Development. Drug linker technology licensed from Seagen, Inc.; mAb produced using POTELLIGENT Technology licensed from BioWa. The NCI-H929 cell line is licensed with the NIH until December 21, 2025. GlaxoSmithKline acknowledges the contributions of Gazdar and Minna for generating this cell line. The Bioware Ultra Cell Line EL4-luc2 was obtained from Caliper Life Sciences, Inc. (catalog No. 124088). The use and transfer of this product and derivatives thereof are limited by the terms and conditions set by Caliper Life Sciences, Inc., which additionally contain limited use statements from Promega Corporation and The Regents of the University of California (see http://www.caliperls.com/assets/017/7513.pdf).

The costs of publication of this article were defrayed in part by the payment of page charges. This article must therefore be hereby marked *advertisement* in accordance with 18 U.S.C. Section 1734 solely to indicate this fact.

Received January 12, 2021; revised May 10, 2021; accepted June 29, 2021; published first July 12, 2021.

References

1. Sakuishi K, Apetoh L, Sullivan JM, Blazar BR, Kuchroo VK, Anderson AC. Targeting Tim-3 and PD-1 pathways to reverse T cell exhaustion and restore anti-tumor immunity. J Exp Med 2010;207:2187–94.
2. Hoos A. Development of immuno-oncology drugs - from CTLA4 to PD1 to the next generations. Nat Rev Drug Discov 2016;15:235–47.
3. Gramaglia I, Weinberg AD, Lemon M, Croft M. Ox-40 ligand: a potent costimulatory molecule for sustaining primary CD4 T cell responses. J Immunol 1998;161:6510–7.
4. Mahoney KM, Rennert PD, Freeman GJ. Combination cancer immunotherapy and new immunomodulatory targets. Nat Rev Drug Discov 2015;14:561–84.
5. Wargo JA, Reuben A, Cooper ZA, Oh KS, Sullivan RJ. Immune effects of chemotherapy, radiation, and targeted therapy and opportunities for combination with immunotherapy. Semin Oncol 2015;42:601–16.
6. Zamarin D, Postow MA. Immune checkpoint modulation: rational design of combination strategies. Pharmacol Ther 2015;150:23–32.
7. Zitvogel L, Kepp O, Kroemer G. Immune parameters affecting the efficacy of chemotherapeutic regimens. Nat Rev Clin Oncol 2011;8:151–60.
8. Matzinger P. Tolerance, danger, and the extended family. Annu Rev Immunol 1994;12:991–1045.
9. Obeid M, Tesniere A, Ghiringhelli F, Fimia GM, Apetoh L, Perfettini JL, et al. Calreticulin exposure dictates the immunogenicity of cancer cell death. Nat Med 2007;13:54–61.
10. Semino C, Angelini G, Poggi A, Rubartelli A. NK/iDC interaction results in IL-18 secretion by DCs at the synaptic cleft followed by NK cell activation and release of the DC maturation factor HMGB1. Blood 2005;106:609–16.
11. Kazama H, Ricci JE, Herndon JM, Hoppe G, Green DR, Ferguson TA. Induction of immunological tolerance by apoptotic cells requires caspase-dependent oxidation of high-mobility group box-1 protein. Immunity 2008;29:21–32.
12. Mizumoto N, Gao J, Matsushima H, Ogawa Y, Tanaka H, Takashima A. Discovery of novel immunostimulants by dendritic-cell-based functional screening. Blood 2005;106:3082–9.
13. Tanaka H, Matsushima H, Mizumoto N, Takashima A. Classification of chemotherapeutic agents based on their differential *in vitro* effects on dendritic cells. Cancer Res 2009;69:6978–86.
14. Tanaka H, Matsushima H, Nishibu A, Clausen BE, Takashima A. Dual therapeutic efficacy of vinblastine as a unique chemotherapeutic agent capable of inducing dendritic cell maturation. Cancer Res 2009;69:6987–94.
15. Darce JR, Arendt BK, Wu X, Jelinek DF. Regulated expression of BAFF-binding receptors during human B cell differentiation. J Immunol 2007;179:7276–86.
16. Montes-Moreno S, Montalban C, Piris MA. Large B-cell lymphomas with plasmablastic differentiation: a biological and therapeutic challenge. Leuk Lymphoma 2012;53:185–94.
17. Elsawa SF, Novak AJ, Grote DM, Ziesmer SC, Witzig TE, Kyle RA, et al. B-lymphocyte stimulator (BLyS) stimulates immunoglobulin production and malignant B-cell growth in Waldenstrom macroglobulinemia. Blood 2006;107:2882–8.
18. Endo T, Nishio M, Enzler T, Cottam HB, Fukuda T, James DF, et al. BAFF and APRIL support chronic lymphocytic leukemia B-cell survival through activation of the canonical NF-kappaB pathway. Blood 2007;109:703–10.
19. Lee L, Bounds D, Paterson J, Herledan G, Sully K, Seestaller-Wehr LM, et al. Evaluation of B cell maturation antigen as a target for antibody drug conjugate mediated cytotoxicity in multiple myeloma. Br J Haematol 2016;174:911–22.
20. Tai YT, Mayes PA, Acharya C, Zhong MY, Cea M, Cagnetta A, et al. Novel anti-B-cell maturation antigen antibody-drug conjugate (GSK2857916) selectively induces killing of multiple myeloma. Blood 2014;123:3128–38.
21. Tai YT, Anderson KC. Targeting B-cell maturation antigen in multiple myeloma. Immunotherapy 2015;7:1187–99.
22. Muller P, Martin K, Theurich S, Schreiner J, Savic S, Terszowski G, et al. Microtubule-depolymerizing agents used in antibody-drug conjugates induce antitumor immunity by stimulation of dendritic cells. Cancer Immunol Res 2014;2:741–55.
23. Muller P, Kreuzaler M, Khan T, Thommen DS, Martin K, Glatz K, et al. Trastuzumab emtansine (T-DM1) renders HER2+ breast cancer highly susceptible to CTLA-4/PD-1 blockade. Sci Transl Med 2015;7:315ra188.
24. Sistigu A, Yamazaki T, Vacchelli E, Chaba K, Enot DP, Adam J, et al. Cancer cell-autonomous contribution of type I interferon signaling to the efficacy of chemotherapy. Nat Med 2014;20:1301–9.
25. Martin K, Muller P, Schreiner J, Prince SS, Lardinois D, Heinzelmann-Schwarz VA, et al. The microtubule-depolymerizing agent ansamitocin P3 programs dendritic cells toward enhanced anti-tumor immunity. Cancer Immunol Immunother 2014;63:925–38.
26. Fucikova J, Kralikova P, Fialova A, Brtnicky T, Rob L, Bartunkova J, et al. Human tumor cells killed by anthracyclines induce a tumor-specific immune response. Cancer Res 2011;71:4821–33.
27. Zappasodi R, Pupa SM, Ghedini GC, Bongarzone I, Magni M, Cabras AD, et al. Improved clinical outcome in indolent B-cell lymphoma patients vaccinated with autologous tumor cells experiencing immunogenic death. Cancer Res 2010;70:9062–72.

28. Ghiringhelli F, Apetoh L, Tesniere A, Aymeric L, Ma Y, Ortiz C, et al. Activation of the NLRP3 inflammasome in dendritic cells induces IL-1beta-dependent adaptive immunity against tumors. Nat Med 2009;15:1170–8.
29. Michaud M, Martins I, Sukkurwala AQ, Adjemian S, Ma Y, Pellegatti P, et al. Autophagy-dependent anticancer immune responses induced by chemotherapeutic agents in mice. Science 2011;334:1573–7.
30. Apetoh L, Ghiringhelli F, Tesniere A, Obeid M, Ortiz C, Criollo A, et al. Toll-like receptor 4-dependent contribution of the immune system to anticancer chemotherapy and radiotherapy. Nat Med 2007;13:1050–9.
31. Steinman RM, Banchereau J. Taking dendritic cells into medicine. Nature 2007; 449:419–26.
32. Rieder CL, Maiato H. Stuck in division or passing through: what happens when cells cannot satisfy the spindle assembly checkpoint. Dev Cell 2004;7: 637–51.
33. Mahalingaiah PK, Ciurlionis R, Durbin KR, Yeager RL, Philip BK, Bawa B, et al. Potential mechanisms of target-independent uptake and toxicity of antibody-drug conjugates. Pharmacol Ther 2019;200:110–25.
34. Farooq AV, Esposti SD, Popat R, Thulasi P, Lonial S, Nooka AK, et al. Corneal epithelial findings in patients with multiple myeloma treated with antibody-drug conjugate belantamab mafodotin in the pivotal, randomized, DREAMM-2 study. Ophthalmol Ther 2020;9:889–911.
35. Zhao H, Atkinson J, Gulesserian S, Zeng Z, Nater J, Ou J, et al. Modulation of macropinocytosis-mediated internalization decreases ocular toxicity of antibody-drug conjugates. Cancer Res 2018;78:2115–26.
36. Wei WZ, Jacob JB, Zielinski JF, Flynn JC, Shim KD, Alsharabi G, et al. Concurrent induction of antitumor immunity and autoimmune thyroiditis in CD4+ CD25+ regulatory T cell-depleted mice. Cancer Res 2005;65:8471–8.
37. Jacob JB, Kong YC, Nalbantoglu I, Snower DP, Wei WZ. Tumor regression following DNA vaccination and regulatory T cell depletion in neu transgenic mice leads to an increased risk for autoimmunity. J Immunol 2009;182: 5873–81.
38. Bates SE. Multiple myeloma: multiplying therapies. Clin Cancer Res 2016;22:5418.
39. Leblay N, Maity R, Hasan F, Neri P. Deregulation of adaptive T cell immunity in multiple myeloma: insights into mechanisms and therapeutic opportunities. Front Oncol 2020;10:636.
40. Trudel S, Lendvai N, Popat R, Voorhees PM, Reeves B, Libby EN, et al. Targeting B-cell maturation antigen with GSK2857916 antibody-drug conjugate in relapsed or refractory multiple myeloma (BMA117159): a dose escalation and expansion phase 1 trial. Lancet Oncol 2018;19:1641–53.
41. Trudel S, Lendvai N, Popat R, Voorhees PM, Reeves B, Libby EN, et al. Antibody-drug conjugate, GSK2857916, in relapsed/refractory multiple myeloma: an update on safety and efficacy from dose expansion phase I study. Blood Cancer J 2019;9:37.
42. Lonial S, Lee HC, Badros A, Trudel S, Nooka AK, Chari A, et al. Belantamab mafodotin for relapsed or refractory multiple myeloma (DREAMM-2): a two-arm, randomised, open-label, phase 2 study. Lancet Oncol 2020;21: 207–21.
43. Rios-Doria J, Harper J, Rothstein R, Wetzel L, Chesebrough J, Marrero A, et al. Antibody-drug conjugates bearing pyrrolobenzodiazepine or tubulysin payloads are immunomodulatory and synergize with multiple immunotherapies. Cancer Res 2017;77:2686–98.
44. Wculek SK, Cueto FJ, Mujal AM, Melero I, Krummel MF, Sancho D. Dendritic cells in cancer immunology and immunotherapy. Nat Rev Immunol 2020;20: 7–24.
45. Zitvogel L, Kepp O, Senovilla L, Menger L, Chaput N, Kroemer G. Immunogenic tumor cell death for optimal anticancer therapy: the calreticulin exposure pathway. Clin Cancer Res 2010;16:3100–4.
46. Garg AD, Nowis D, Golab J, Vandenabeele P, Krysko DV, Agostinis P. Immunogenic cell death, DAMPs and anticancer therapeutics: an emerging amalgamation. Biochim Biophys Acta 2010;1805:53–71.
47. Multhoff G, Mizzen L, Winchester CC, Milner CM, Wenk S, Eissner G, et al. Heat shock protein 70 (Hsp70) stimulates proliferation and cytolytic activity of natural killer cells. Exp Hematol 1999;27:1627–36.
48. Kroemer G, Galluzzi L, Kepp O, Zitvogel L. Immunogenic cell death in cancer therapy. Annu Rev Immunol 2013;31:51–72.
49. Zitvogel L, Galluzzi L, Kepp O, Smyth MJ, Kroemer G. Type I interferons in anticancer immunity. Nat Rev Immunol 2015;15:405–14.
50. Pfirschke C, Engblom C, Rickelt S, Cortez-Retamozo V, Garris C, Pucci F, et al. Immunogenic chemotherapy sensitizes tumors to checkpoint blockade therapy. Immunity 2016;44:343–54.